10.1109/ULTSYM.2009.0479

Algorithm for Estimating the Attenuation Slope from Backscattered Ultrasonic Signals

Alexander Haak[1], Zachary T. Hafez[1], Janelle J. Anderson[3], Maria-Teresa Herd[3], Kibo Nam[3], Ernest L. Madsen[3], Timothy A. Bigelow[2], Timothy J. Hall[3], William D. O'Brien, Jr.[1]
[1]Bioacoustics Research Laboratory, Department of Electrical and Computer Engineering
University of Illinois at Urbana-Champaign, Urbana, IL, 61801
[2]Department of Electrical and Computer Engineering, Department of Mechanical Engineering
Iowa State University, Ames, IA 50011
[3]Department of Medical Physics, University of Wisconsin-Madison, Madison, WI, 53706
Email: ahaak@illinois.edu

***Abstract*—In vivo attenuation slope measurements usually utilize the backscattered signal from pulse/echo ultrasound. In this work the down shift of the center frequency of an emitted ultrasound pulse with penetration depth is utilized to estimate the attenuation slope. A diffraction correction of the focused ultrasound source is performed by measuring the reflection from a planar surface positioned throughout the depth of focus. A focused single element transducer with a measured center frequency of 8.2 MHz and a fractional band width of 72% was used to interrogate four tissue mimicking phantoms. The scatterers in the tissue mimicking phantoms were glass spheres embedded in a gelatin/milk matrix. In one set of the phantoms, the backscattering strength was varied; in the other set of phantoms the attenuation slope was varied. The attenuation slope (AS_{BS}) was estimated using pulse/echo data obtained by scanning the phantoms. The "true" attenuation slope (AS_{Thru}) was obtained from two independent insertion loss measurements performed at two different laboratories. The relative error of AS_{BS} was investigated for different regions of interest (ROI) for all phantoms. Three different axial and lateral ROI sizes were tested. It was observed that the average relative error (average over all four phantoms) changed by less than three percent when the lateral size of the ROI was decreased by seventy percent. The axial size of the ROI was changed by thirty percent whereas the average error changed by less then three percent.**

I. Introduction

The ultrasonic attenuation slope (AS; unit: dB/cm-MHz) can be utilized as a parameter in quantitative ultrasound imaging to characterize tissue. Therefore, the AS may be used as a tool to diagnose diseases. For *in vivo* applications it is necessary to utilize the backscattered radio frequency (RF) signal. In previous work, the downshift of the center frequency of an ultrasound pulse or the decrease of the spectral amplitude (spectral difference) with depth was used to estimate the AS. Fink et al. [1] used a short time Fourier transformation to calculate the down shift of the spectral centroid with depth. Yao et al. [2] applied narrow band filters to the backscattered signal and calculated the attenuation from the decrease of the spectral amplitude with depth. However, in addition to the attenuation loss due to the medium there is diffraction of the ultrasound source. While diffraction may be neglected for weakly focused sources most sources require correcting for diffraction prior to finding the AS. Yao et al. [2] introduced a reference phantom method to correct for system dependent parameters including diffraction. Madsen et al. [3] calculated the field generated by focused ultrasound sources that can be used to correct for diffraction. Bigelow et al. [4] used a Gaussian approximation of the field near to the focus to correct for diffraction.

The accuracy and robustness of the AS estimates using the backscattered signal depends on several factors. Spatial speckle noise modifies the spectrum of received ultrasound pulses that results in noisy spectra. Spatial averaging can reduce this effect but decreases the lateral resolution of the AS estimates. Furthermore, the axial resolution is limited by a minimum truncation window length in order to compute stable spectra.

In this work we present an algorithm that utilized the spectral down shift with depth to estimate AS. Tissue mimicking phantoms were scanned with a single element transducer in pulse/echo mode. The assumed to be "true" AS was measured, using insertion loss techniques, at two different laboratories and compared to the AS estimates using the backscattered signal technique (BST). The robustness of the BST was tested by varying the number of RF lines used to compute the average spectral amplitudes and by changing the the axial section length used to truncate the RF lines.

II. Methodology

A. Phantoms

Four tissue mimicking phantoms were manufactured. The phantoms consisted of a gelatin/milk background material in which glass bead inclusions were embedded. This mixture was put into an acryl cylinder that had on top and bottom Saran wrap serving as acoustic windows. One set of phantoms had constant AS but the backscattering strength (BS) was varied by about 3 dB. The other set of phantoms had constant BS but the attenuation was varied by about 0.2 dB/cm-MHz. The phantom properties are shown in Table I.

B. Insertion Loss Measurements

For all tissue mimicking phantoms two insertion loss measurement procedures were performed at two different labo-

TABLE I
THE BACKSCATTERING STRENGTH (BS) WAS VARIED BY PHANTOMS OF THE FIRST SET BUT THE ATTENUATION SLOPE (AS) WAS KEPT CONSTANT. PHANTOMS OF SECOND SET HAD CONSTANT BACKSCATTERING STRENGTH BUT THE ATTENUATION SLOPE WAS VARIED.

	Set I		**Set II**	
Label	Low BS Const. AS	High BS Const. AS	Const. BS Low AS	Const. BS High AS
Sphere diameter (μm)	13 - 23	13 - 23	13 - 23	13 - 23
# density sphere $\left(\times 10^6 cm^{-3}\right)$	0.3	1.1	0.6	0.6
Target AS (dB/cm-MHz)	0.5	0.5	0.5	0.7

ratories. At the University of Illinois at Urbana-Champaign (UIUC) a broadband method was used. All experiments were performed in a tank with degassed water. A single element transducer (Panametrics model V321), center frequency 8.2 MHz, was used as a transmitter. A micropositioning system (Daedal, Inc., Harrisburg, PA) was used to move the transmitter focus yielding to a maximum amplitude response at a PVDF membrane hydrophone (Marconi Model Y-34-6543, Chelmsford, UK). The amplitude responses with and without the phantom in the propagation path were recorded. The insertion loss spectrum was obtained from the difference of the two power spectra (dB) with and without sample in place. The AS (dB/cm-MHz) was calculated by dividing the insertion loss spectrum by the sample thickness (cm) and frequency (MHz).

At the University of Wisconsin (UW) an narrow band method was used. A matched pair of focused transducer (Panametrics V320), center frequency 7.5 MHz, were coaxial aligned. One of the transducer (transmitter) was driven by pulser receiver (Panametrics model 5800) whereas the other transducer worked as a receiver. The transmitted signals were recorded using an oscilloscope (LeCroy Waverunner LT342 500MHz) with and without the phantom in the acoustic path. The attenuation coefficient (dB/cm) was estimated by a log spectral difference technique [6].

C. Insertion Loss Data Processing

The AS obtained from the two insertion loss measurements were assumed to have only a random error that was described by a normal distribution. The assumed to be "true" AS (AS_{Thru}) was calculated by taking the average AS of both measurements. An error analysis was performed to estimate the overall uncertainty of AS_{Thru}.

D. Data Acquisition Backscatter Technique

A single element transducer (Panametrics model V321), center frequency 8.2 MHz, was mounted in a positioning system (Daedal, Inc., Harrisburg, PA). The transducer was driven by a pulser/receiver (Panametrics, Waltham, Massachusetts) and received echoes were digitized (PDA-14, Signatec, CA) and stored to a personal computer. A reference scan was performed by moving the transducer axially towards a planar Plexiglas reflector with a step size of half of the wavelength. At each scan step the reflection of the reflector was recorded over the field's depth of focus (DOF). The tissue mimicking phantoms were placed in a tank filled with degassed water. The transducer focus was positioned approximately 9 mm beneath the sample surface. Eighty adjacent RF lines were acquired by moving the transducer laterally with a step size (400 μm) of approximately half the transducer beam width. This procedure was repeated five times in order to obtain five independent B-mode slices.

TABLE II
ROI SIZES OF THE DIFFERENT AVERAGE SPECTRAL AMPLITUDES USING 15, 25 AND 50 ADJACENT RF LINES. THE SECTION LENGTH WAS KEPT CONSTANT AT 3 MILLIMETER.

Number of RF lines	15	25	50
Lateral ROI (mm)	6	10	20
Axial ROI (mm)	10.5	10.5	10.5

E. Backscatter Data Processing

Within the DOF six sections with an overlap of fifty percent were axially truncated. The average spectral amplitude using several adjacent RF lines was calculated for each section. Diffraction correction was performed by dividing the average spectral amplitude ($|V_{Samp}(f,z_0)|$) by the reference spectral amplitude ($|V_{Ref}(f,z_0)|$), obtained from the reference scan, corresponding to the same depth. This spectral ratio was multiplied by the reference spectral amplitude ($|V_{Ref}(f,z_F)|$) obtained at the transducer focus (z_F) (Equation 1).

$$|V_{cor}(f,z_0)| = \frac{|V_{Samp}(f,z_0)|}{|V_{Ref}(f,z_0)|}\,|V_{Ref}(f,z_F)| \qquad (1)$$

We assume that the corrected spectral amplitude ($|V_{Cor}(f,z_0)|$) can be approximated by a Gaussian function and a local attenuation term (Equation 2),

$$|V_{cor}(f,z_0)| \approx \exp\left[-\frac{(f-f_{Peak})^2}{2\sigma^2} - 2\alpha_{Local}(f)\,z_0\right] \qquad (2)$$

where $\alpha_{Local}(f)$ is the local attenuation in Np/cm. The center frequency (f_{Peak}) and bandwidth (σ) of the corrected spectral amplitudes were obtained by fitting a Gaussian function for each section. The AS was then calculated by using Equation 3 assuming linear frequency dependency of $\alpha_{Local}(f)$,

$$AS = -\frac{1}{2\widetilde{\sigma}^2}\frac{\partial f_{Peak}}{\partial z_0} \qquad (3)$$

where (z_0) is the relative distance to the focus and ($\widetilde{\sigma}$) is the average bandwidth obtained from all six sections.

In order to test the robustness of the BST algorithm the number of RF lines and the length of the sections to compute the average spectra were varied. In Table II the resulting region of interest (ROI) sizes are shown for using 15, 25 and 50 RF lines to compute the average spectra. Secondly, the length of the individual sections was varied by 2.0, 2.5 and 3.0 mm, corresponding to approximately 15, 12 and 10 wavelengths respectively whereas the number of RF lines (50) was kept constant. The resulting ROI sizes are shown in Table III.

TABLE III
ROI SIZES OF THE DIFFERENT AVERAGE SPECTRAL AMPLITUDES USING 2.0, 2.5 AND 3.0 MILLIMETER LONG SECTIONS TO COMPUTE AVERAGE SPECTRA. THE NUMBER OF RF LINES USED WAS KEPT CONSTANT TO FIFTY.

Section length (mm)	2.0	2.5	3.0
Lateral ROI (mm)	20	20	20
Axial ROI (mm)	7.0	8.8	10.5

III. RESULTS

The estimated AS_{Thru} and the AS estimates using the BST for the three different investigated lateral ROI sizes are shown in Figure 1. In Figure 2 the AS estimates using the BST are shown for the three different axial ROI sizes.

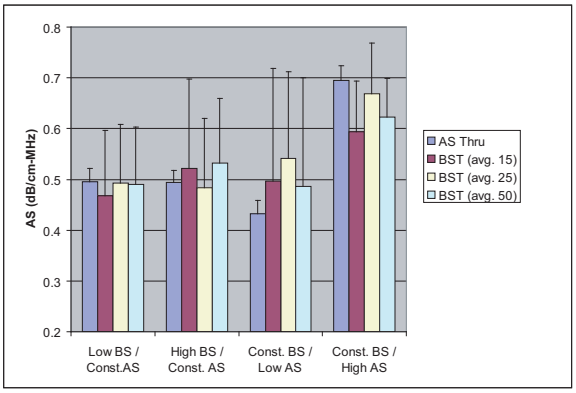

Fig. 1. Estimated AS for the four different tissue mimicking phantoms. The lateral ROI size, 6, 10 and 20 mm, was varied by using 15, 25 and 50 adjacent RF lines to compute the average spectral amplitude. The length of the truncation window was kept constant at 3.0 mm. The error bars represent twice the standard deviation yielding to a confidence interval of approximately 95 percent.

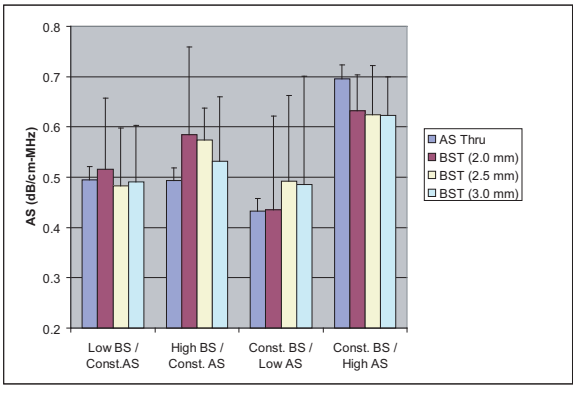

Fig. 2. Estimated AS for the four different tissue mimicking phantoms. The axial ROI size, 7.0, 8.8 and 10.5 mm was varied by using three different truncation windows (2.0, 2.5 and 3.0 mm) for each section to compute the average spectral amplitude. The number of RF lines used to compute the average spectra was kept constant to 50 RF lines. The error bars represent twice the standard deviation yielding to a confidence interval of approximately 95 percent.

IV. DISCUSSION

Insertion loss measurements are well characterized and there is currently no better method to estimate AS [7]. An overall uncertainty assessment was performed for both insertion loss measurements. The highest overall uncertainty for the assumed to be "true" AS (AS_{Thru}) was calculated to be 11% and the average uncertainty for AS_{Thru} was 7%.

The error for the AS estimates using the BST relative to AS_{Thru} for the different lateral ROI sizes is shown in Figure 3. There is no apparent dependency of the relative error on the number of RF lines used for the average spectra because the estimated uncertainties are overlapping (Figure 3). The relative precision (twice the standard deviation) of the BST for the different lateral ROI sizes is shown in Figure 4. The precision of the AS estimates using the BST is degrading with decreasing number of RF lines to compute the average spectra except for the phantom *Const. BS/Low AS*. The increased error for the phantom *Const. BS/Low AS* (Figure 3) may be due to a shortcoming during data acquisition which is indicated by a worse precision (Figure 4) for this phantom. Another explanation for the increased error for this phantom may be shortcomings during the phantom manufacturing process. Clusters of scattering sites (deviations from the uniform distributed scatterer locations) will increase the local attenuation in this area of the phantom. A larger lateral ROI size may include such a region whereas a smaller lateral ROI size does not include such an region. This would alter the AS estimate for different lateral ROI sizes. Scanning all phantoms with a clinical scanner, Sonix RP (Ultrasonix, British Columbia, Canada), using a 10 MHz probe did not show any evidence of clustering of the scatterers.

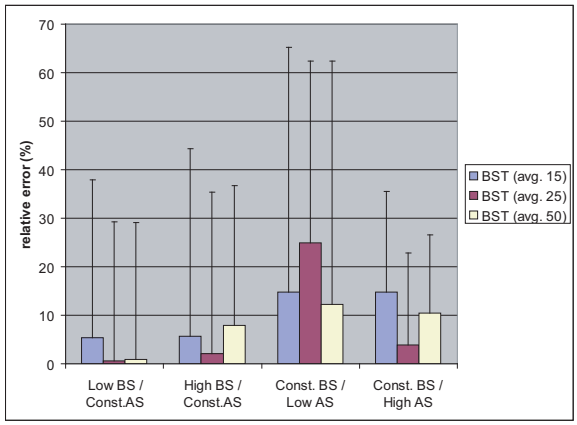

Fig. 3. Relative error of BST estimates using 15, 25 and 50 RF lines to compute the average spectra. The error bars represent the sum of the relative uncertainties obtained from the insertion loss measurements (AS_{Thru}) and the uncertainties of the AS estimates using the BST yielding to a 95 percent confidence interval.

In Figure 5 the relative error for the BST AS-estimates relative to AS_{Thru} for the different axial ROI sizes are shown. The errors for all phantoms and axial ROI sizes are less then 20%. There was no dependency of the relative error on the axial ROI size observed for the ROI sizes tested. The precision

for the AS estimates using different axial ROI sizes are plotted in Figure 6. No dependency of the precision on the axial ROI size was observed for the ROI sizes tested (Figure 6).

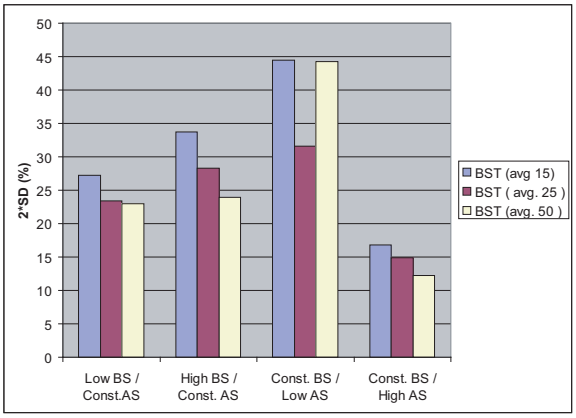

Fig. 4. Precision, twice the standard deviation (SD), in percent for 15, 25 and 50 RF lines used to compute the average spectra.

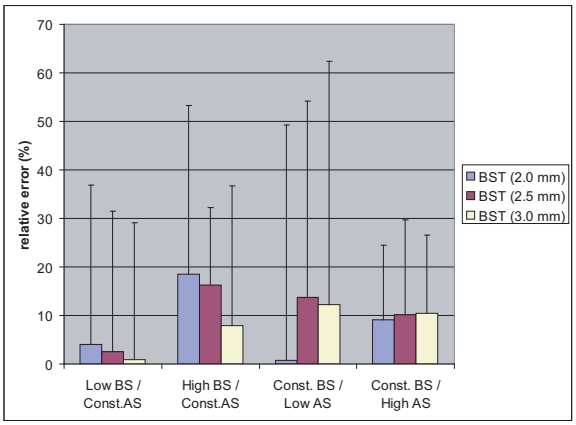

Fig. 5. Relative error of BST estimates using a section length of 2.0, 2.5 and 3.0 mm (resulting in an axial ROI size of 7.0, 8.8 and 10.5 mm respectively) to compute the average spectra. The error bars represent the sum of the relative uncertainties obtained from the insertion loss measurements (AS_{Thru}) and the uncertainties of the AS estimates using the BST.

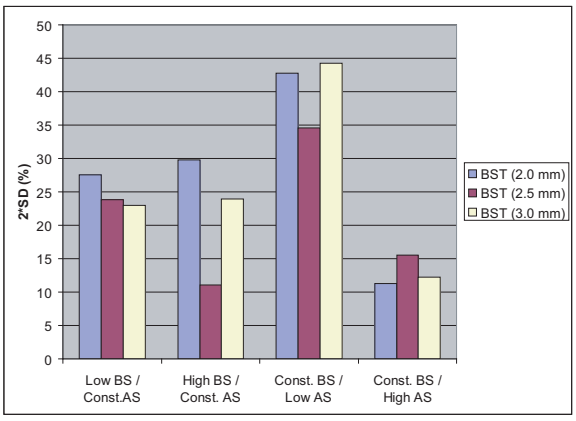

Fig. 6. Precision, twice the standard deviation (SD), in percent for an axial ROI size of 7.0, 8.8 and 10.5 mm used to compute the average spectra.

V. Conclusion

The proposed BS technique was applied to four tissue mimicking phantoms and the AS was estimated for different ROI sizes. The AS estimates, using the BST, were compared to the assumed to be ”true” AS obtained from insertion loss measurements. The average error for all phantoms was 10.2, 7.9 and 7.9% for 15, 25 and 50 RF lines, respectively. There was a decreased precision of the AS estimates when the lateral ROI size was decreased by approximately 5 to 13%. The average errors for all phantoms varying the axial ROI size were 8.1, 10.6 and 7.9% for a window length of 2.0, 2.5 and 3.0 mm, respectively. There was no dependency of the relative error as a function of either the lateral or the axial ROI size. An increased precision could be observed for increasing lateral ROI sizes but not for larger axial ROI sizes.

Acknowledgment

This work was supported by NIH Grant CA111289.

References

[1] M. Fink, F. Hottier and J.F. Cardoso, *Ultrasonic Signal Processing for In vivo Attenuation Measurement: Short time Fourier Analysis*, Ultrasonic Imaging 5, 117-135 (1983).

[2] L. X. Yao, J. A. Zagzebski, and E. L. Madsen, *Backscatter coefficient measurements using a reference phantom to extract depth-dependent instrumentation factors*, Ultrasonic Imaging 12, 58-70 (1990).

[3] E. L. Madsen, M. M. Goodsitt, and J. A. Zagzebski, *Continuous waves generated by focused radiators*, j. Acoust. Soc. Am. 70(5), 1508-1517 (1981).

[4] T. A. Bigelow, B. L. McFarlin, M. L. Oelze and W. D. O'Brien Jr., *In vivo ultrasonic attenuation slope estimates for detecting cervical ripening in rats: Preliminary results*, J. Acoust. Soc. Am. 123 (3), 1794-1800 (2008).

[5] H. Kim and T. Varghese, *Hybrid Spectral Domain Method for Attenuation Slope Estimation*, Ultrasound in Med. & Biol. 34, 1808-1819 (2008).

[6] R. Kuc and M. Schwartz, *Estimating the acoustic attenuation coefficient slope for liver from reflected ultrasound signals*, IEEE Trans Son Ultrason, 353-362, (1979).

[7] C. R. Hill, J. C. Bamber and G. R. ter Haar, *Physical Principles of Medical Ultrasonics* (John Wiley & Sons, Ltd, 2004).